HYPERSINGULAR INTEGRAL EQUATIONS FOR THE SOLUTION OF PENNY-SHAPED INTERFACE CRACK PROBLEMS

Bahattin Kilic and Erdogan Madenci

HYPERSINGULAR INTEGRAL EQUATIONS FOR THE SOLUTION OF PENNY-SHAPED INTERFACE CRACK PROBLEMS

BAHATTIN KILIC AND ERDOGAN MADENCI

Based on the theory of elasticity, previous analytical solutions concerning a penny-shaped interface crack employ the derivative of the crack surface opening displacements as the primary unknowns, thus leading to singular integral equations with Cauchy-type singularity. The solutions to the resulting integral equations permit only the determination of stress intensity factors and energy release rate, and do not directly provide crack opening and sliding displacements. However, the crack opening and sliding displacements are physically more meaningful and readily validated against the finite element analysis predictions and experimental measurements. Therefore, the present study employs crack opening and sliding as primary unknowns, rather than their derivatives, and the resulting integral equations include logarithmic-, Cauchy-, and Hadamard-type singularities. The solution to these singular integral equations permits the determination of not only the complex stress intensity factors but also the crack opening displacements.

1. Introduction

During fabrication, the presence of dissimilar material interfaces is unavoidable, and they are prone to imperfections. If the interface is too strong to delaminate, the cracking occurs in the weakest of the adjoining materials. On the other hand, delamination may initiate along the interface for a sufficiently weak interface. Based on the concept of fracture mechanics, the singular character of the stresses near the crack front and the stress intensity factors are important in failure prediction.

Within the realm of the theory of elasticity both for a plane and a penny-shaped crack, there exist numerous analytical studies addressing the oscillating stress singularity and stress intensity factors at an interface crack. Extensive discussion on the treatment of an oscillatory singular stress field near the interface crack was given by Erdogan [1997] and recently by Kilic et al. [2006]. The most common solution method of integral transformations includes the presence of singular stresses at the crack front by treating the derivatives of the crack opening displacements as primary unknowns, leading to a system of Cauchy-type singular integral equations. Solutions to these singular integral equations can be achieved by techniques developed by Erdogan [1969], Erdogan and Gupta [1971a; 1971b], Miller and Keer [1985], and Kabir et al. [1998] that yield the stress intensity factors.

Because of the nature of the primary unknowns in the singular integral equations, previous studies concerning interface cracks concern the calculation of the stress intensity factors or the energy release rate rather than the crack surface displacements. However, the crack surface displacements are physically more meaningful and easier to compare against experimental measurements and finite element solutions that fail to provide accurate stress intensity and energy release rate without resorting to a refined mesh

or a special crack tip element. Furthermore, this approach is more viable for consideration of three-dimensional crack problems within the realm of mixed boundary value problems as indicated by Kaya [1984].

The construction of the solution to the integral equations concerning a plane crack is relatively simpler than that for a penny-shaped crack, and is discussed in detail by Kilic et al. [2006]. For a penny-shaped interface crack between two dissimilar elastic materials that are semiinfinite in extent, Kassir and Bregman [1972] constructed the exact solution to the stress intensity factors utilizing analytic functions introduced by [Mossakovski and Rybka 1964]. This problem also attracted the attention of Erdogan [1965], Willis [1972], and Lowengrub and Sneddon [1974]. Erdogan [1965] obtained the singular stress field near the crack front by using the integral representation of displacement components suggested by Harding and Sneddon [1945] while considering the derivatives of crack surface displacements as primary unknowns in the derivation of Cauchy-type singular integral equations. However, Willis [1972] constructed the solution through the use of the Radon transform of the relative displacement of crack surfaces. Adopting the solution method by Erdogan [1965]. Lowengrub and Sneddon [1974], Keer et al. [1978], and Farris and Keer [1985] also examined the singular character of stresses of a penny-shaped interface crack. However, the numerical evaluation of the integrals in these studies is fraught with complete regularization of the kernels by ignoring the logarithmic singularities and thus the convergence difficulty. Therefore, logarithmic singularities have to be taken into account in the numerical analysis as suggested by Ozturk and Erdogan [1996].

Unlike previous studies, the present study considers the crack surface displacements, rather than their derivatives, as primary unknowns in the singular integral equations. After the regularization of the kernels, the resulting integral equations include logarithmic-, Cauchy-, and Hadamard-type singularities. Solution to these singular integral equations leads to the determination of not only stress intensity factors but also crack opening displacements, which are more desirable for experimental comparisons. This approach also naturally provides the complex stress intensity factors required for the energy release rate calculation given by Malyshev and Salganik [1965]. Within the context of solution methods available in the literature, this study for the first time presents an approach for constructing the solution of a singular integral equation in the presence of the combination of Hadamard, Cauchy, and logarithmic singularities. Although this approach provides accurate crack opening and sliding displacements, it does not remove the oscillatory singular stress field near the interface crack.

The description of the geometry and the crack configurations are shown in the next section. The solution method and the numerical analysis of the singular integral equations with the Hadamard-type singularity are described in the subsequent sections. The numerical results concern the energy release rate calculations and the crack surface displacements.

2. Problem statement

As shown in Figure 1, a circular crack with radius a is situated at the interface between two material layers with thicknesses h_1 and h_2. The crack lies on the (r, θ) plane of the cylindrical coordinate system (r, θ, z) whose origin is located at the center of the crack. The regions along the positive and negative z-directions are S_2 and S_1, respectively. The material in each region is isotropic, elastic, and homogeneous, with shear moduli μ_1 and μ_2, and Poisson's ratios ν_1 and ν_2. The bounding surface of region S_2 is
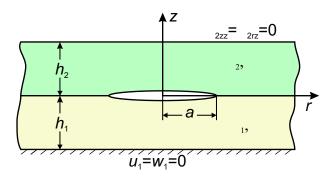
Figure 1. The circular crack geometry between two bonded dissimilar material layers.

traction free and that of S_1 is constrained from displacements. The crack surfaces are subjected to an internal pressure of p_0. This configuration was considered previously by Farris and Keer [1985] while using the derivatives of the crack surface displacements as primary unknowns. It reduces to the case considered by Goldstein and Vainshelbaum [1976] by allowing h_1 to approach infinity.

By invoking the kinematic and stress-strain relations into the equilibrium equations in the absence of the body forces and time dependence, the displacement equilibrium equations under axisymmetric conditions for each region can be expressed as

$$(\kappa_i + 1)\left\{\frac{\partial^2 u_i}{\partial r^2} + \frac{1}{r}\frac{\partial u_i}{\partial r} - \frac{1}{r^2}u_i + \frac{\partial^2 w_i}{\partial r \partial z}\right\} + (\kappa_i - 1)\left\{\frac{\partial^2 u_i}{\partial z^2} - \frac{\partial^2 w_i}{\partial r \partial z}\right\} = 0,$$

$$(\kappa_i + 1)\left\{\frac{\partial^2 u_i}{\partial r \partial z} + \frac{1}{r}\frac{\partial u_i}{\partial z} + \frac{\partial^2 w_i}{\partial^2 z}\right\} - (\kappa_i - 1)\left\{\frac{\partial^2 u_i}{\partial r \partial z} - \frac{\partial^2 w_i}{\partial r^2} + \frac{1}{r}\frac{\partial u_i}{\partial z} - \frac{1}{r}\frac{\partial w_i}{\partial r}\right\} = 0,$$

(1)

where $\kappa_i = 3 - 4\nu_i$ and u_i and w_i are the radial and vertical components of the displacement vector, respectively. The subscript $i = 1$ represents the substrate and $i = 2$ the film, as shown in Figure 1. From the stress-strain relations along with kinematics, the relevant stress components in cylindrical coordinates under axisymmetric conditions can be expressed as

$$\sigma_{izz} = \frac{2\mu_i}{1 - 2\nu_i}\left\{(1 - \nu_i)\frac{\partial w_i}{\partial z} + \nu_i\left(\frac{\partial u_i}{\partial r} + \frac{u_i}{r}\right)\right\}, \qquad \sigma_{irz} = \mu_i\left(\frac{\partial u_i}{\partial z} + \frac{\partial w_i}{\partial r}\right).$$

Traction free conditions along $z = h_2$ and constrained displacement conditions along $z = -h_1$ require the imposition of conditions

$$\sigma_{2zz}(r, h_2) = 0, \quad \sigma_{2rz}(r, h_2) = 0, \quad u_1(r, -h_1) = 0, \quad w_1(r, -h_1) = 0, \qquad 0 \le r < \infty. \quad (2)$$

Along the interface between regions S_1 and S_2 on the plane of $z = 0$, the continuity of traction and displacement components requires the imposition of

$$\sigma_{1zz}(r, 0) = \sigma_{2zz}(r, 0), \quad \sigma_{1rz}(r, 0) = \sigma_{2rz}(r, 0), \qquad 0 \le r < \infty, \quad (3)$$

$$u_{1zz}(r, 0) = u_{2zz}(r, 0), \quad w_{1zz}(r, 0) = w_{2zz}(r, 0), \qquad a \le r < \infty. \quad (4)$$

Finally, the applied tractions on the upper and lower crack surfaces of the $z = 0^{\pm}$ planes are specified as

$$\sigma_{1zz}(r, 0^-) = \sigma_{2zz}(r, 0^+) = p(r), \quad \sigma_{1rz}(r, 0^-) = \sigma_{2rz}(r, 0^+) = q(r), \qquad 0 \leq r < a. \tag{5}$$

The mathematical boundary value problem then reduces to the determination of the crack opening and sliding displacements, as well as the stress intensity factors and the energy release rate at the crack tip.

3. Solution procedure

The solution procedure involves the use of integral transformation techniques appropriate for mixed boundary value problems. Utilizing the integral representation of the displacement field suggested by Harding and Sneddon [1945] the displacement components in each region are represented by

$$u_i(r, z) = \int_0^\infty d\rho\, F_i(\rho, z)\rho J_1(r\rho), \qquad w_i(r, z) = \int_0^\infty d\rho\, G_i(\rho, z)\rho J_0(r\rho), \tag{6}$$

where J_0 and J_1 are the Bessel functions of the first kind with orders 0 and 1, respectively.

Substituting these integral representations into the displacement equilibrium equations, Equation (1), leads to a coupled system of second-order ordinary differential equations for the auxiliary functions, $F_i(\rho, z)$ and $G_i(\rho, z)$. Their general solution form can be expressed as

$$\begin{bmatrix} F_i(\rho, z) \\ G_i(\rho, z) \end{bmatrix} = A_{i1}e^{-\rho z}\begin{bmatrix} 1 \\ 1 \end{bmatrix} + A_{i2}e^{-\rho z}\begin{bmatrix} z \\ \frac{\kappa_i}{\rho} + z \end{bmatrix} + A_{i3}e^{\rho z}\begin{bmatrix} 1 \\ -1 \end{bmatrix} + A_{i4}e^{\rho z}\begin{bmatrix} z \\ \frac{\kappa_i}{\rho} - z \end{bmatrix}, \tag{7}$$

where $A_{ij}(\rho)$ for $i = 1, 2$ and $j = 1 \ldots 4$ are the unknown coefficients to be determined from the prescribed boundary conditions given by Equations (2)–(5).

Enforcing the boundary conditions specified by Equations (2) and (3) results in

$$2\rho e^{-\rho h_2}A_{21} + (\kappa_2 + 1 + 2\rho h_2)e^{-\rho h_2}A_{22} + 2\rho e^{\rho h_2}A_{23} - (\kappa_2 + 1 - 2\rho h_2)e^{\rho h_2}A_{24} = 0,$$

$$2\rho e^{-\rho h_2}A_{21} + (\kappa_2 - 1 + 2\rho h_2)e^{-\rho h_2}A_{22} - 2\rho e^{\rho h_2}A_{23} + (\kappa_2 - 1 - 2\rho h_2)e^{\rho h_2}A_{24} = 0,$$

$$e^{\rho h_1}A_{11} - h_1 e^{\rho h_1}A_{12} + e^{-\rho h_1}A_{13} - h_1 e^{-\rho h_1}A_{14} = 0,$$

$$e^{\rho h_1}A_{11} + (\kappa_1/\rho - h_1)e^{\rho h_1}A_{12} - e^{-\rho h_1}A_{13} + (\kappa_1/\rho + h_1)e^{-\rho h_1}A_{14} = 0,$$

$$2\mu_2\rho A_{21} + (1 + \kappa_2)\mu_2 A_{22} + 2\mu_2\rho A_{23} - (1 + \kappa_2)\mu_2 A_{24} - 2\mu_1\rho A_{11} - (1 + \kappa_1)\mu_1 A_{12}$$
$$-2\mu_1\rho A_{13} + (1 + \kappa_1)\mu_1 A_{14} = 0,$$

$$2\mu_2\rho A_{21} + (\kappa_2 - 1)\mu_2 A_{22} - 2\mu_2\rho A_{23} + (\kappa_2 - 1)\mu_2 A_{24} - 2\mu_1\rho A_{11} - (\kappa_1 - 1)\mu_1 A_{12}$$
$$+2\mu_1\rho A_{13} - (\kappa_1 - 1)\mu_1 A_{14} = 0. \tag{8}$$

Representing the opening and sliding of the crack surfaces by unknown functions $U(r)$ and $W(r)$ as

$$u_2(r, 0^+) - u_1(r, 0^-) = U(r)H(a - r), \qquad w_2(r, 0^+) - w_1(r, 0^-) = W(r)H(a - r) \tag{9}$$

ensures the continuity of the displacement components, Equation (4), along the interface plane of $z = 0$ and $H(\xi)$ is the Heaviside step function. In lieu of directly imposing the continuity requirement of the displacement components along the interface to simplify the algebraic manipulations, the auxiliary

functions $g_1(r)$ and $g_2(r)$ are introduced in the form

$$g_1(r) = \frac{\partial W}{\partial r}H(a-r), \qquad g_2(r) = \left(\frac{\partial U}{\partial r} + \frac{U}{r}\right)H(a-r), \tag{10}$$

in which the unknown functions $U(r)$ and $W(r)$ are defined in Equation (9). Their explicit form can be obtained by substituting Equations (6) and (7) into Equation (10) as

$$g_1(r) = \int_0^\infty d\rho\rho\Big[\kappa_1(A_{12}+A_{14}) - \kappa_2(A_{22}+A_{24}) + (A_{11}-A_{21}-A_{13}+A_{23})\rho\Big]J_1(\rho r),$$
$$g_2(r) = \int_0^\infty d\rho\rho^2\Big[-A_{11}+A_{21}-A_{13}+A_{23}\Big]J_0(\rho r).$$

Inversion of these equations by using the related Hankel transforms results in

$$G_1(\rho) = -\rho A_{21} - \kappa_2 A_{22} + \rho A_{23} - \kappa_2 A_{24} + \rho A_{11} + \kappa_1 A_{12} - \rho A_{13} + \kappa_1 A_{14},$$
$$G_2(\rho) = \rho A_{21} + \rho A_{23} - \rho A_{11} - \rho A_{13}, \tag{11}$$

in which

$$G_1(\rho) = \int_0^a ds g_1(s)s J_1(s\rho), \qquad G_2(\rho) = \int_0^a ds g_2(s)s J_0(s\rho). \tag{12}$$

In matrix form, the combination of all the boundary conditions given by Equations (8) and (11) can be expressed as

$$\boldsymbol{Ca} = \boldsymbol{b}, \tag{13}$$

in which the explicit forms of $\boldsymbol{C}$, $\boldsymbol{a}$, and $\boldsymbol{b}$ are given in Appendix A. The unknown coefficients A_{ij} with $i = 1, 2$ and $j = 1 \ldots 4$, contained in vector $\boldsymbol{a}$ can be solved for in terms of the unknown auxiliary functions $G_1(\rho)$ and $G_2(\rho)$ contained in vector $\boldsymbol{b}$ in the form

$$A_{ij} = A_{ij}\big(G_1(\rho), G_2(\rho)\big). \tag{14}$$

Although the formulation presented herein only considers boundary conditions of the clamped type on region S_1 and traction free on region S_2, it can easily be extended to include different boundary conditions such as clamped on both regions and traction free on both regions, and their combinations. Imposition of different types of boundary conditions only requires the modification of the matrix $\boldsymbol{C}$ to reflect changes in Equation (2).

The remaining unknown functions $G_1(\rho)$ and $G_2(\rho)$ are determined by enforcing the applied tractions on the crack surfaces given by Equation (5), resulting in

$$\mu_2 \int_0^\infty d\rho\rho\Big[(1+\kappa_2)(A_{24}-A_{22}) - 2\rho(A_{21}+A_{23})\Big]J_0(\rho r) = p(r),$$
$$\mu_2 \int_0^\infty d\rho\rho\Big[(1-\kappa_2)(A_{24}+A_{22}) - 2\rho(A_{21}-A_{23})\Big]J_1(\rho r) = q(r), \tag{15}$$

where the stress components are defined in region S_2, and A_{ij} are already determined by Equation (14).

In order to avoid divergent kernels and to simplify the analysis regarding the asymptotic behavior of the kernels, both sides of Equation (15) are integrated over r while invoking Equation (12), resulting in

$$
\int_0^a ds\, s\, g_1(s) \int_0^\infty d\rho\, H_{11}(\rho) J_1(\rho r) J_1(\rho s) + \int_0^a ds\, s\, g_2(s) \int_0^\infty d\rho\, H_{12}(\rho) J_1(\rho r) J_0(\rho s)
$$
$$
= \frac{1}{r}\left(\int_r p(\lambda)\lambda d\lambda + c_1\right),
$$
$$
\int_0^a ds\, s\, g_1(s) \int_0^\infty d\rho\, H_{21}(\rho)(1 - J_0(\rho r)) J_1(\rho s) + \int_0^a ds\, s\, g_2(s) \int_0^\infty d\rho\, H_{22}(\rho)(1 - J_0(\rho r)) J_0(\rho s)
$$
$$
= \int_r q(\lambda)d\lambda + c_2,
$$

(16)

in which $H_{ij}(\rho)$, with $i, j = 1, 2$, are defined in terms of the coefficients of $\boldsymbol{C}^{-1}$ in Appendix A, and c_i represents the integration constants. As the integration variable ρ approaches infinity, the kernels $H_{ij}(\rho)$ possess the asymptotic behavior

$$
\lim_{\rho \to \infty} H_{11}(\rho) = -\lim_{\rho \to \infty} H_{22}(\rho) = \gamma_{11} = \frac{\mu_1\mu_2\big(\mu_1(1+\kappa_2) + \mu_2(1+\kappa_1)\big)}{(\mu_2 + \kappa_2\mu_1)(\mu_1 + \kappa_1\mu_2)},
$$
$$
\lim_{\rho \to \infty} H_{12}(\rho) = -\lim_{\rho \to \infty} H_{21}(\rho) = \gamma_{12} = \frac{\mu_1\mu_2\big(\mu_1(1-\kappa_2) - \mu_2(1-\kappa_1)\big)}{(\mu_2 + \kappa_2\mu_1)(\mu_1 + \kappa_1\mu_2)}.
$$

By considering the asymptotic behavior of kernels, using $\gamma = -\gamma_{12}/\gamma_{11}$ Equation (16) can be rewritten as

$$
-\gamma \int_0^a ds\, s\, g_2(s) \int_0^\infty d\rho\, J_1(\rho r) J_0(\rho s) + \int_0^a ds\, s\, g_2(s) \int_0^\infty d\rho\, \frac{H_{12}(\rho) - \gamma_{12}}{\gamma_{11}} J_1(\rho r) J_0(\rho s)
$$
$$
+ \int_0^a ds\, s\, g_1(s) \int_0^\infty d\rho\, J_1(\rho r) J_1(\rho s) + \int_0^a ds\, s\, g_1(s) \int_0^\infty d\rho\, \frac{H_{11}(\rho) - \gamma_{11}}{\gamma_{11}} J_1(\rho r) J_1(\rho s)
$$
$$
= \frac{1}{\gamma_{11} r}\left(\int_r p(\lambda)\lambda d\lambda + C_1\right),
$$
$$
\gamma \int_0^a ds\, s\, g_1(s) \int_0^\infty d\rho\,(1 - J_0(\rho r)) J_1(\rho s) + \int_0^a ds\, s\, g_1(s) \int_0^\infty d\rho\, \frac{H_{21}(\rho) + \gamma_{12}}{\gamma_{11}}(1 - J_0(\rho r)) J_1(\rho s)
$$
$$
- \int_0^a ds\, s\, g_2(s) \int_0^\infty d\rho\,(1 - J_0(\rho r)) J_0(\rho s) + \int_0^a ds\, s\, g_2(s) \int_0^\infty d\rho\, \frac{H_{22}(\rho) + \gamma_{11}}{\gamma_{11}}(1 - J_0(\rho r)) J_0(\rho s)
$$
$$
= \frac{1}{\gamma_{11}}\left(\int_r q(\lambda)d\lambda + C_2\right),
$$

(17)

After differentiating these equations term by term with respect to r, application of integration by parts to replace the unknown functions $g_1(s)$ and $g_2(s)$ with the unknown functions $W(s)$ and $U(s)$ and the

use of Equation (A.1) when appropriate leads to

$$\frac{1}{\pi}\int_0^a ds \frac{W(s)}{(s-r)^2} + \frac{1}{2\pi r}\int_0^a ds \frac{W(s)}{s-r} - \frac{1}{8\pi r^2}\int_0^a ds\, W(s)\ln|s-r| + \int_0^a ds\, W(s)K_{11}(r,s)$$

$$+ \int_0^a ds\, U(s)K_{12}(r,s) - \gamma\frac{U(r)}{r} - \gamma\frac{\partial U(r)}{\partial r} = \frac{1}{\gamma_{11}}p(r), \quad (18)$$

$$\frac{1}{\pi}\int_0^a ds \frac{U(s)}{(s-r)^2} + \frac{1}{2\pi r}\int_0^a ds \frac{U(s)}{s-r} + \frac{3}{8\pi r^2}\int_0^a ds\, U(s)\ln|s-r| + \int_0^a ds\, W(s)K_{21}(r,s)$$

$$+ \int_0^a ds\, U(s)K_{22}(r,s) + \gamma\frac{\partial W(r)}{\partial r} = \frac{1}{\gamma_{11}}q(r), \quad (19)$$

in which the kernels are defined as

$$K_{11}(r,s) = m_{11}(r,s) - \frac{1}{\pi(s-r)^2} - \frac{1}{2\pi r(s-r)} + \frac{\ln|s-r|}{8\pi r^2} - s\int_0^\infty d\rho\, \frac{H_{11}(\rho)-\gamma_{11}}{\gamma_{11}}\rho^2 J_0(\rho r)J_0(\rho s),$$

$$K_{12}(r,s) = s\int_0^\infty d\rho\, \frac{H_{12}(\rho)-\gamma_{12}}{\gamma_{11}}\rho^2 J_0(\rho r)J_1(\rho s),$$

$$\tag{20}$$

$$K_{21}(r,s) = -s\int_0^\infty d\rho\, \frac{H_{21}(\rho)+\gamma_{12}}{\gamma_{11}}\rho^2 J_1(\rho r)J_0(\rho s),$$

$$K_{22}(r,s) = m_{22}(r,s) - \frac{1}{\pi(s-r)^2} - \frac{1}{2\pi r(s-r)} - \frac{3\ln|s-r|}{8\pi r^2} + s\int_0^\infty d\rho\, \frac{H_{22}(\rho)+\gamma_{11}}{\gamma_{11}}\rho^2 J_1(\rho r)J_1(\rho s),$$

where $m_{11}(r,s)$ and $m_{22}(r,s)$ are given in Appendix A. Multiplying Equation (19) by $i = \sqrt{-1}$ and adding to Equation (18) leads to their combination as

$$\frac{1}{\pi}\int_0^a ds \frac{f(s)}{(s-r)^2} + \frac{1}{2\pi r}\int_0^a ds \frac{f(s)}{s-r} + \frac{1}{8\pi r^2}\int_0^a ds\, f(s)\ln|s-r| - \frac{1}{4\pi r^2}\int_0^a ds\, f^*(s)\ln|s-r|$$

$$+ \int_0^a ds\, K_1(r,s)f(s) + \int_0^a ds\, K_2(r,s)f^*(s) + i\frac{\gamma}{2r}f(r) - i\frac{\gamma}{2r}f^*(r) + i\gamma\frac{df(r)}{dr} = \frac{p(r)+iq(r)}{\gamma_{11}}, \quad (21)$$

where the unknown complex-valued function is $f(r) = W(r) + iU(r)$, with its complex conjugate represented by f^*. The complex-valued kernels K_1 and K_2 are defined as

$$K_1(r,s) = \tfrac{1}{2}\Big(K_{11}(r,s) + K_{22}(r,s) - i\big[K_{12}(r,s) - K_{21}(r,s)\big]\Big),$$

$$K_2(r,s) = \tfrac{1}{2}\Big(K_{11}(r,s) - K_{22}(r,s) + i\big[K_{12}(r,s) + K_{21}(r,s)\big]\Big).$$

In addition to the presence of Hadamard-, Cauchy-, and logarithmic-type singularities, the dominant part of the kernels $K_1(r,s)$ and $K_2(r,s)$ in Equation (21) becomes unbounded as both r and s approach zero. Kernels of this type are analogous to the generalized Cauchy-type kernels [Erdogan 1978]. The unknown function $f(r)$ can be defined as

$$f(r) = \frac{F(r)}{(a-r)^\alpha r^\beta},$$

in which $F(r)$ is an unknown bounded function. By using the function-theoretic method of Muskhelishvili [1992] and the properties of hypersingular integral equations described by Kaya [1984], Kaya and

Erdogan [1987], Ioakimidis [1988b; 1988a; 1990], and later by Chan et al. [2003] and Kilic et al. [2006], the strength of the singularities α and β can be obtained as

$$\alpha = -\tfrac{1}{2} + i\omega, \qquad \beta = 0, \quad \text{with} \quad \omega = \frac{1}{2\pi} \ln\left(\frac{1-\gamma}{1+\gamma}\right).$$

For an interface crack, the complex stress intensity factor that is equivalent to that of Erdogan and Gupta [1971a; 1971b] and Kassir and Bregman [1972] can be defined as

$$k_1 + ik_2 = \lim_{r \to a} (r-a)^{-\alpha^*} 2^{-\alpha} (\sigma_{zz} + i\sigma_{rz}),$$

where α^* is the complex conjugate of α. This allows the stress intensity factor to be re-expressed as

$$\frac{1}{\gamma_{11}\sqrt{1-\gamma^2}}\big(k_1(a) + ik_2(a)\big) = -2\alpha \lim_{r \to a}(r-a)^{\alpha}(2a)^{\alpha^*} f(r) = -2^{-2\alpha}\alpha\sqrt{a}F(a).$$

In the limiting case of both h_1 and h_2 approaching infinity, the stress intensity factor for constant pressure can be expressed analytically using the formula given by Kassir and Bregman [1972] as

$$k_1 + ik_2 = 2p_0\sqrt{\frac{a}{\pi}}\frac{\Gamma(2-i\omega)}{\Gamma(1/2-i\omega)}, \tag{22}$$

in which Γ represents the gamma function. Knowing the stress intensity factors permits the evaluation of the phase angle, ψ, equivalent to that of Jensen [1998], in the form

$$\tan\psi = \frac{\mathrm{Im}\big((k_1 + ik_2)h_2^{-i\omega}\big)}{\mathrm{Re}\big((k_1 + ik_2)h_2^{-i\omega}\big)}.$$

As introduced by Erdogan and Gupta [1971a; 1971b], the energy release rate can be related to the stress intensity factors in the form

$$\mathcal{G} = \frac{\pi}{2}\frac{(\mu_1 + \kappa_1\mu_2)(\mu_2 + \kappa_2\mu_1)}{\mu_1\mu_2\big[(1+\kappa_1)\mu_2 + (1+\kappa_2)\mu_1\big]}(k_1^2 + k_2^2).$$

4. Numerical analysis of integral equations

By introducing $r = a(x+1)/2$, $s = a(t+1)/2$, for $-1 \le (x,t) \le 1$, the integro-differential equation, Equation (21), is normalized as

$$\frac{2}{\pi a}\int_{-1}^{1}dt\frac{g(t)}{(t-x)^2} + \frac{1}{2\pi r}\int_{-1}^{1}dt\frac{g(t)}{t-x} + \frac{a}{16\pi r^2}\int_{-1}^{1}dt\,g(t)\ln|t-x| - \frac{a}{8\pi r^2}\int_{-1}^{1}dt\,f^*(t)\ln|t-x|$$

$$+ \int_{-1}^{1}dt\,M_1(x,t)g(t) + \int_{-1}^{1}dt\,M_2(x,t)g^*(t) + i\frac{\gamma}{2r}g(x) - i\frac{\gamma}{2r}g^*(x) + i\frac{2\gamma}{a}\frac{dg(x)}{dx} = \frac{p(r)+iq(r)}{\gamma_{11}}, \tag{23}$$

where $g(x) = f(a(x+1)/2)$ and M_1 and M_2 are defined as

$$M_1(x,t) = \tfrac{1}{2}\Big(M_{11}(x,t) + M_{22}(x,t) - i\frac{a}{2}\big[K_{12}(r,s) - K_{21}(r,s)\big]\Big),$$

$$M_2(x,t) = \tfrac{1}{2}\Big(M_{11}(x,t) - M_{22}(x,t) + i\frac{a}{2}\big[K_{12}(r,s) + K_{21}(r,s)\big]\Big),$$

where

$$M_{11}(x,t) = \frac{a}{2}m_{11}(r,s) - \frac{2}{\pi a(t-x)^2} - \frac{1}{2\pi r(t-x)} + \frac{a\ln|t-x|}{16\pi r^2} - \frac{as}{2}\int_0^\infty d\rho\,\frac{H_{11}(\rho)-\gamma_{11}}{\gamma_{11}}\rho^2 J_0(\rho r)J_0(\rho s),$$

$$M_{22}(x,t) = \frac{a}{2}m_{22}(r,s) - \frac{2}{\pi a(t-x)^2} - \frac{1}{2\pi r(t-x)} - \frac{3a\ln|t-x|}{16\pi r^2} + \frac{as}{2}\int_0^\infty d\rho\,\frac{H_{22}(\rho)+\gamma_{11}}{\gamma_{11}}\rho^2 J_1(\rho r)J_1(\rho s).$$

Furthermore, the normalized unknown function $g(x)$ can be rewritten as

$$g(x) = \frac{G(x)}{(1-x)^\alpha}, \tag{24}$$

where the unknown auxiliary function $G(x)$ is bounded.

The kernels $M_1(x,t)$ and $M_2(x,t)$ appearing in Equation (23) involve the computation of infinite integrals. These integrals are evaluated by using the modified form of Filon's numerical scheme in order to account for the oscillations arising from the Bessel functions of the first kind. This integration algorithm is outlined in Appendix B. The complexity of the kernels in Equation (23) requires that the singular integral equations be solved numerically. The solution procedure involves the reduction of the integro-differential equations with Hadamard-, Cauchy-, and logarithmic-type singularities to a system of linear algebraic equations using the collocation technique introduced by Miller and Keer [1985] and later extended by Quan [1991] to include the generalized Cauchy kernel, and by Kabir et al. [1998] to include Hadamard- and logarithmic-type singularities.

In this technique, the quadrature interval $[-1, 1]$ is partitioned into a series of subintervals. The integration points, t_k, at the ends and midpoint of each subinterval are shown in Figure 2. The collocation points x_n are defined at the midpoint of two consecutive integration points.

The unknown function $G(t)$ in Equation (24) is approximated over each subinterval $t_{2k-1} \le t \le t_{2k+1}$, for $k = 1, \ldots, N$, by quadratic Lagrange interpolation polynomials, which are given as

$$G(t) \approx \left[\frac{(t-t_{2k})^2}{h_k^2} - \frac{(t-t_{2k})}{h_k}\right]\frac{G_{2k-1}}{2} + \left[1 - \frac{(t-t_{2k})^2}{h_k^2}\right]G_{2k} + \left[\frac{(t-t_{2k})^2}{h_k^2} + \frac{(t-t_{2k})}{h_k}\right]\frac{G_{2k+1}}{2},$$

where $G_k = G(t_k)$ and $h_k = (t_{2k+1} - t_{2k-1})/2$.

Figure 2. Discretization of the quadrature interval.

Approximation of the unknown function $G(x)$ permits the discretization of Equation (23) as

$$
\sum_{m=1}^{2N+1} \left[\frac{2}{\pi a} w_m^H(x_n) G_m + \frac{1}{2\pi r_n} w_m^C(x_n) G_m + \frac{a}{16\pi r_n^2} w_m^L(x_n) G_m - \frac{a}{8\pi r_n^2} w_m^{L^*}(x_n) G_m^* + M_1(x_n, t_m) v_m G_m \right.
$$

$$
\left. + M_1(x_n, t_m) v_m^* G_m^* \right] + \sum_{j=1}^{3} \left[i \frac{\gamma}{2r_n(1-x_n)^\alpha} \left(B_j G_{I+j} - B_j G_{I+j}^* \right) + i \frac{2\gamma}{a(1-x_n)^{1+\alpha}} B_j G_{I+j} \right]
$$

$$
+ i \frac{2\gamma}{a(1-x_n)^\alpha} \sum_{j=1}^{M} D_j(h_n) G_{L+j} = \frac{1}{\gamma_{11}} (p(x_n) + i q(x_n)), \quad (25)
$$

where N is the number of subintervals for the unknown function $G(x)$ and $r_n = a(x_n + 1)/2$. The singular weight functions, $w_m^H(x)$, $w_m^C(x)$, $w_m^L(x)$, and v_m, as well as I and B_j, are given by Kabir et al. [1998] and L and D_j are defined by Kilic et al. [2006]. The variable with a superscript * denotes its complex conjugate.

Because this discretization results in a number of unknowns G_m, which are one more than the number of equations, an additional constraint equation becomes necessary in order to achieve a unique solution to Equation (25). However, the nature of this solution method does not yield any additional constraint equations based on the physics of the problem. Therefore, the necessary equation is introduced in an artificial way in order to achieve a unique solution, as suggested by Kabir et al. [1998] and Kilic et al. [2006]. It is obtained by multiplying the integro-differential equation given by (23) by $r^2(1-x^2)^{3/2}$ and integrating over x between -1 and 1. After changing the order of integrations, performing the appropriate algebraic manipulations leads to the normal and discretized forms

$$
\int_{-1}^{1} dt \, K_{1c}(t) g(t) + K_{2c}(t) g^*(t) = \tilde{g}, \qquad \sum_{m=1}^{2N+1} K_{1c}(t_m) v_m G_m + K_{2c}(t_m) v_m^* G_m^* = \tilde{g}.
$$

The details of the algebraic manipulations, as well as the definitions of $\tilde{g}$, $K_{1c}(t)$, and $K_{2c}(t)$, are given in Appendix C.

Furthermore, the examination of the kernels reveals that they approach zero as $t \to -1$ ($s \to 0$) for $x \neq -1$ ($r \neq 0$). Therefore, $G_1 = G(-1)$ disappears as $t \to -1$, for $x \neq -1$, making the first column equal to zero in the construction of the algebraic equations formed by Equation (25); thus leading to a singular coefficient matrix. To make the system of equations nonsingular, the first row of the coefficient matrix is replaced by imposing the conditions of zero radial displacement and zero slope of transverse displacement at the center of the crack, that is,

$$
\text{Im}[g(t = -1)] = 0, \qquad \text{Re}\left[\frac{\partial g(t = -1)}{\partial t} \right] = 0.
$$

The discrete form of the singular integral equation and constraint equation can be cast into the form $A_{nm} G_m = g_m$ for $m, n = 1, \ldots, 2N+1$, where the unknown vector has form $\mathbf{G}^T = \{ G_1, G_2, \ldots, G_{2N+1} \}$.

N	k_1	k_2
3	0.630	-0.0929
5	0.634	-0.0979
10	0.635	-0.0992
20	0.635	-0.0995
30	0.635	-0.0996

Table 1. Convergence of stress intensity factors.

5. Numerical results

To establish the number of subintervals associated with the unknown functions, the problem of a penny-shaped crack at the interface of two semiinfinite dissimilar materials under unit pressure is considered. Material properties are the same as those given by Kassir and Bregman [1972], and Young's modulus and Poisson's ratio have numerical values of 3×10^7 psi and 0.3 for the material at the upper half and 10^7 psi and 0.22 for material at the lower half. The analytical solution using Equation (22) can be computed as $k_1 + i k_2 = 0.635 - 0.0996i$. The convergence of the stress intensity factors as a function of number of integration points is presented in Table 1. As demonstrated in this table, the numerical technique used in this study gives 3-digit accuracy, as compared to analytical solution using only 30 integration points. Therefore, in the solution of the integral equations, the number of subintervals associated with the unknown function is chosen to be 100. The material properties used in this analysis are the same as those given by Farris and Keer [1985] and Wan et al. [2003], and their values are presented in Table 2. In this table, the aluminum layer of 7075-T6 Al represents the rigid substrate, and the polymeric materials represent the film.

The validity of the results of the present analysis was established by comparing the crack opening and sliding displacements with the finite element predictions. Finite element analysis was conducted using PLANE42 elements of the commercially available package ANSYS®. The PLANE42 element can be used as an axisymmetric element with four nodes, having two degrees of freedom at each node. In the finite element discretization, the radius of the material layer is 20 times that of the crack radius in order to represent infinite length in radial direction. The finite element mesh has 50 equally spaced nodes in the radial direction along the crack surface. The elements surrounding the crack tip are of traditional elements without special treatment of the singularity at the crack tip.

Material	Modulus (MPa)	Poisson's Ratio
7075-T6 Al Alloy	7.1705×10^4	0.33
Polymeric Material	4.0×10^3	0.35
Solithane 113	3.447	0.499
PMMA	2.758	0.495

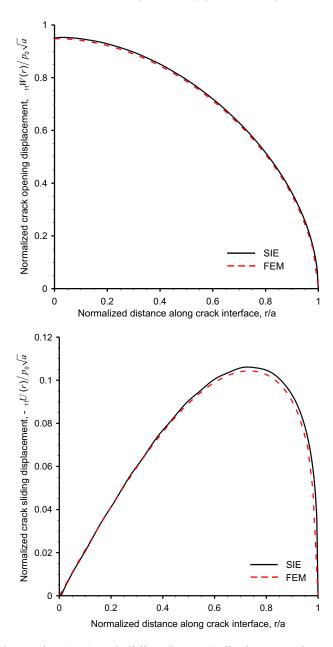**Table 2.** Mechanical properties of materials.

Figure 3. Crack opening (top) and sliding (bottom) displacement between 7075-T6 Al substrate and polymeric film for $h_2/h_1 = 1$.

In the validation of the present analysis against the finite element predictions, the film thickness is taken to be equal to that of the substrate, $h_2/h_1 = 1$, and the crack length is equal to that of the thin film thickness, $h_2/a = 1$. As shown in Figure 3, predictions of the present analysis are in remarkable agreement with the finite element results. To capture the effects of thin film thickness on the fracture parameters, the ratio of thin film thickness to crack radius h_2/a is varied ranging from 0.4 to 4.
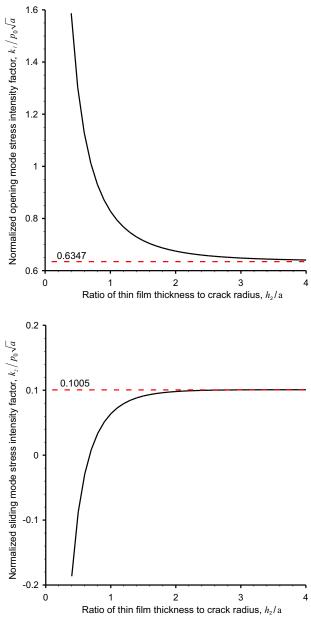
Figure 4. Opening (top) and sliding (bottom) mode stress intensity factor for a crack between 7075-T6 Al substrate and polymeric film for $h_2/h_1 = 1$.

As observed in Figures 4–5, the energy release rate and stress intensity factors for the opening and sliding modes increase as the ratio of h_2/a decreases. The complex stress intensity factor approaches the limiting value given by Kassir and Bregman [1972] as the ratio of h_2/a increases. The central deflection as a function of the ratio h_2/a is shown in Figure 6.
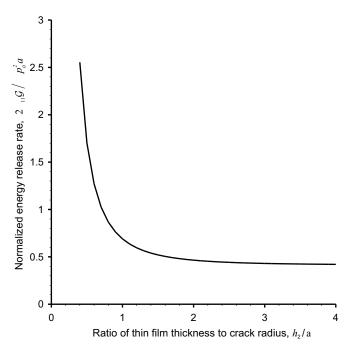
Figure 5. Energy release rate at a crack front between 7075-T6 Al substrate and polymeric film for $h_2/h_1 = 1$.
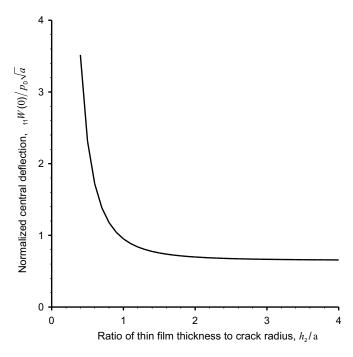

Figure 6. Central deflection of a crack between 7075-T6 Al substrate and polymeric film for $h_2/h_1 = 1$.
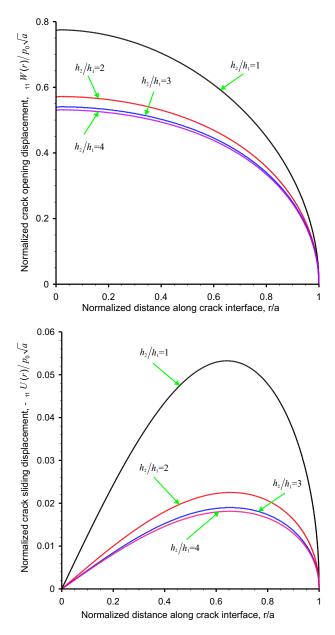
Figure 7. Crack opening (top) and sliding (bottom) displacement between Solithane 113 and PMMA material layers.

If the adhesive between the two material layers has a comparable modulus, it should be explicitly included in the analysis. The present analysis can be used to model such a material system. To illustrate this capability, the adherend material PMMA is attached to a rigid substrate using the adhesive material Solithane 113. The results are presented for four different adherend-to-adhesive thickness ratios
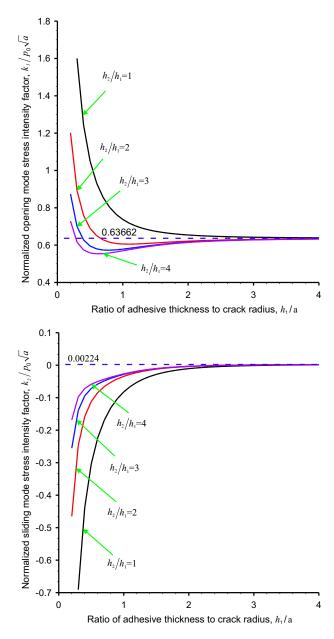
Figure 8. Opening (top) and sliding (bottom) mode stress intensity factor for a crack between Solithane 113 and PMMA material layers.

of $h_2/h_1 = 1$ and 4 by an increment of 1. The crack opening and sliding displacements are shown in Figure 7. The stress intensity factors and energy release rate increase as h_1/a decreases for $h_2/h_1 = 1$, as presented in Figures 8–9. However, for $h_2/h_1 = 4$, the stress intensity factor for the opening mode and energy release rate have a minimum at $h_1/a \approx 0.75$, as also pointed out by Farris and Keer [1985], but the stress intensity factor for the sliding mode increases as h_1/a decreases. Similar behavior is observed for
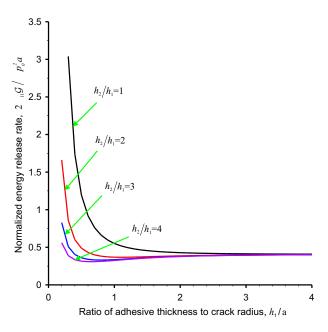
Figure 9. Energy release rate at a crack front between Solithane 113 and PMMA material layers.
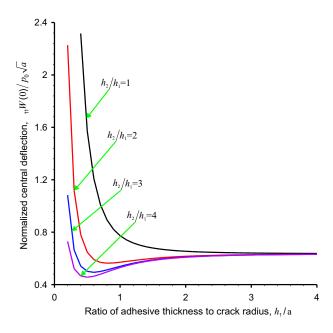
Figure 10. Central deflection of a crack between Solithane 113 and PMMA material layers.

$h_2/h_1 = 2$ and $h_2/h_1 = 3$. As the h_1/a ratio increases, the complex stress intensity factor approaches that given by Kassir and Bregman [1972]. The crack opening displacements at the center are also presented in Figure 10.

6. Conclusions

By using the linear theory of elasticity and applying the appropriate mixed boundary conditions, the interface penny-shaped crack problem is reduced to a boundary-value problem. The formulation of this boundary-value problem leads to a singular integral equation of the Hadamard-, Cauchy-, and logarithmic-type, which is solved numerically to directly obtain the crack opening and sliding displacements, as well as the stress intensity factors and energy release rate. Numerical results are validated by comparing against the crack opening and sliding displacements obtained from the finite element analysis. The limiting value of the complex stress intensity factor for which both the substrate and film thicknesses approach infinity is also in agreement with the analytical benchmark solution. The present analysis can be used to investigate the interface toughness between not only the film and rigid substrate but also the film and adhesive, which have comparable magnitudes of elastic moduli. Within the context of solution methods available in the literature, this study, for the first time, presents an approach for constructing the solution of a singular integral equation in the presence of a combination of Hadamard, Cauchy, and logarithmic singularities.

Appendix A

The matrix C in Equation (13) is given by

$$
\begin{bmatrix}
-\rho & -\kappa_2 & \rho & -\kappa_2 & \rho & \kappa_1 & -\rho & \kappa_1 \\
\rho & 0 & \rho & 0 & -\rho & 0 & -\rho & 0 \\
2\mu_2\rho & (1+\kappa_2)\mu_2 & 2\mu_2\rho & -(1+\kappa_2)\mu_2 & -2\mu_1\rho & -(1+\kappa_1)\mu_1 & -2\mu_1\rho & (1+\kappa_1)\mu_1 \\
2\mu_2\rho & (\kappa_2-1)\mu_2 & -2\mu_2\rho & (\kappa_2-1)\mu_2 & -2\mu_1\rho & -(\kappa_1-1)\mu_1 & 2\mu_1\rho & -(\kappa_1-1)\mu_1 \\
0 & 0 & 0 & 0 & e^{\rho h_1} & -h_1 e^{\rho h_1} & e^{-\rho h_1} & -h_1 e^{-\rho h_1} \\
0 & 0 & 0 & 0 & e^{\rho h_1} & \left(\frac{\kappa_1}{\rho}-h_1\right)e^{\rho h_1} & -e^{-\rho h_1} & \left(\frac{\kappa_1}{\rho}+h_1\right)e^{-\rho h_1} \\
2\rho e^{-\rho h_2} & (\kappa_2+1+2\rho h_2)e^{-\rho h_2} & 2\rho e^{\rho h_2} & -(\kappa_2+1-2\rho h_2)e^{\rho h_2} & 0 & 0 & 0 & 0 \\
2\rho e^{-\rho h_2} & (\kappa_2-1+2\rho h_2)e^{-\rho h_2} & -2\rho e^{\rho h_2} & (\kappa_2-1-2\rho h_2)e^{\rho h_2} & 0 & 0 & 0 & 0
\end{bmatrix}.
$$

The vectors a and b, also from Equation (11), are given by $a^T = [A_{21}\ A_{22}\ A_{23}\ A_{24}\ A_{11}\ A_{12}\ A_{13}\ A_{14}]$, and $b^T = [G_1(\rho)\ G_2(\rho)\ 0\ 0\ 0\ 0\ 0\ 0]$, where superscript T represents the transpose. The kernels appearing in infinite integrals in Equation (16) are expressed as

$$
H_{11}(\rho) = \mu_2\big[(1+\kappa_2)(B_{41} - B_{21}) - 2\rho(B_{11} + B_{31})\big],
$$
$$
H_{12}(\rho) = \mu_2\big[(1+\kappa_2)(B_{42} - B_{22}) - 2\rho(B_{12} + B_{32})\big],
$$
$$
H_{21}(\rho) = \mu_2\big[(1-\kappa_2)(B_{41} + B_{21}) - 2\rho(B_{11} - B_{31})\big],
$$
$$
H_{22}(\rho) = \mu_2\big[(1-\kappa_2)(B_{42} + B_{22}) - 2\rho(B_{12} - B_{32})\big],
$$

where the coefficients $B_{ij} = C_{ij}^{-1}$.

The closed-form evaluation of certain integrals that are used in Equations (17)–(19) are

$$\int_0^\infty d\rho\, J_1(\rho r) J_1(\rho s) = \frac{2}{\pi} \begin{cases} \frac{1}{s}[K(s/r) - E(s/r)], & s < r, \\ \frac{1}{r}[K(r/s) - E(r/s)], & s > r, \end{cases}$$

$$\int_0^\infty d\rho\, J_0(\rho r) J_0(\rho s) = \frac{2}{\pi} \begin{cases} \frac{1}{r} K(s/r), & s < r, \\ \frac{1}{s} K(r/s), & s > r, \end{cases} \tag{A.1}$$

$$s \int_0^\infty d\rho\rho\, J_m(\rho r) J_m(\rho s) = \delta(r - s),$$

where $\delta(r)$ is the Dirac delta function. The complete elliptic integrals of the first and second kind, K and E, respectively, are defined by

$$K(m) = \int_0^{\pi/2} \frac{d\theta}{\sqrt{1 - m^2 \sin^2 \theta}}, \qquad E(m) = \int_0^{\pi/2} d\theta \sqrt{1 - m^2 \sin^2 \theta}, \tag{A.2}$$

where $-1 \le m \le 1$. The functions $m_{11}(r, s)$ and $m_{22}(r, s)$ appearing in Equation (20) are defined as

$$m_{11}(r, s) = \begin{cases} \frac{2s\left(2r^2 E(s/r) + (s^2 - r^2)K(s/r)\right)}{\pi r (s^2 - r^2)^2}, & s < r, \\ \frac{4s^2 E(r/s) - 2(s^2 - r^2)K(r/s)}{\pi (s^2 - r^2)^2}, & s > r, \end{cases} \qquad m_{22}(r, s) = \begin{cases} \frac{2\left((s^2 + r^2)E(s/r) + (s^2 - r^2)K(s/r)\right)}{\pi(s^2 - r^2)^2}, & s < r, \\ \frac{2s\left((s^2 + r^2)E(r/s) - (s^2 - r^2)K(r/s)\right)}{\pi r (s^2 - r^2)^2}, & s > r, \end{cases}$$

in which K and E are the complete first and second kind elliptic integrals, respectively, and their explicit forms are given by Equation (A.2).

Appendix B

The approximate evaluation of the integrals of type $I(r, s, t; a, b) = \int_a^b dx\, f(x)\chi_1(rx)\chi_2(sx)\chi_3(tx)$, in which χ_i, with $i = 1, 2, 3$, are functions that possibly have oscillatory behavior (for example, Bessel functions) and $f(x)$ being smooth in the interval $[a, b]$ can be achieved by

$$I(r, s, t; a, b) = \sum_{j=1}^N I_j(r, s, t; x_{2j-1}, x_{2j+1}), \tag{B.1}$$

in which N is the number of subintervals in the interval $[a, b]$. Although it is not necessary for the subintervals to have the same abscissa, the subinterval lengths are taken as equal for simplicity, leading to equal integration intervals $x_{2j-1} - x_{2j+1} = (b - a)/N$. I_j is defined as

$$I_j(r, s, t; x_{2j-1}, x_{2j+1}) = \int_{x_{2j-1}}^{x_{2j+1}} dx f(x)\chi_1(rx)\chi_2(sx)\chi_3(tx). \tag{B.2}$$

Over the subinterval $[x_{2j-1}, x_{2j+1}]$, this integral can be approximated as $I_j(r, s, t; x_{2j-1}, x_{2j+1}) = w_{2j-1} f(x_{2j-1}) + w_{2j} f(x_{2j}) + w_{2j+1} f(x_{2j+1})$, where w_{2j-1}, w_{2j}, and w_{2j+1} are the integration weights. They are determined by assuming a quadratic variation of the product of the functions χ_i, with $i = 1, 2, 3$,

in the interval $[x_{2j-1}, x_{2j+1}]$ with $n = 0, 1, 2$ such that

$$\int_{x_{2j-1}}^{x_{2j+1}} dx\, x^n \chi_1(rx)\chi_2(sx)\chi_3(tx) = x_{2j-1}^n w_{2j-1} + x_{2j}^n w_{2j} + x_{2j+1}^n w_{2j+1} = R_n. \tag{B.3}$$

In matrix form, these equations are rewritten as

$$\begin{bmatrix} 1 & 1 & 1 \\ x_{2j-1} & x_{2j} & x_{2j+1} \\ x_{2j-1}^2 & x_{2j}^2 & x_{2j+1}^2 \end{bmatrix} \begin{bmatrix} w_{2j-1} \\ w_{2j} \\ w_{2j+1} \end{bmatrix} = \begin{bmatrix} R_0 \\ R_1 \\ R_2 \end{bmatrix}, \tag{B.4}$$

from which the weights are computed after the evaluation of the expressions for $R_n(r, s, t; x_{2j-1}, x_{2j+1})$. This is achieved by defining the variable $x = az + x_{2j}$, with $a = (x_{2j+1} - x_{2j-1})/2$, and by approximating the functions χ_i, with $i = 1, 2, 3$, in the integrals in Equation (B.2) using the Chebyshev polynomials of the first kind as

$$\chi_i(p(az + x_{2j})) = \sum_{m=0}^{M_i} b_m T_m(z), \quad \text{with} \quad p \in \{r, s, t\}, \tag{B.5}$$

in which M_i, with $i = 1, 2, 3$, is the highest degree of Chebyshev polynomial used in the approximation and the coefficients are given by

$$b_m = \frac{c}{M_i} \left(\chi_i(p(az_0 + x_{2j})) + (-1)^m \chi_i(p(az_{M_i} + x_{2j})) + 2 \sum_{k=1}^{M_i-1} \chi_i(p(az_k + x_{2j})) \cos \frac{mk\pi}{M_i} \right),$$

in which $z_k = \cos(k\pi/M_i)$, $c = 1$ for $m = 1, \ldots, M_i - 1$ and $c = 1/2$ for $m = 0, M_i$. Substitution from Equation (B.5) into Equation (B.3) with $n = 0, 1, 2$ results in

$$R_n = a \sum_{p=0}^{M_1} \sum_{r=0}^{M_2} \sum_{s=0}^{M_3} b_{1p} b_{2r} b_{3s} \int_{-1}^{1} dz (az + x_{2j})^n T_p(z) T_r(z) T_s(z),$$

This expression permits the explicit evaluation of R_n with the identities [Balkan 1995]

$$\int_{-1}^{1} dz\, T_p(z) T_r(z) T_s(z) = F(p, r, s, 1),$$

$$\int_{-1}^{1} dz\, z T_p(z) T_r(z) T_s(z) = \frac{F(p, r, s, 2)}{2},$$

$$\int_{-1}^{1} dz\, z^2 T_p(z) T_r(z) T_s(z) = \frac{F(p, r, s, 3) + F(p, r, s, 1)}{4},$$

in which

$$F(p, r, s, n) = \tfrac{1}{2} \left(\frac{s+n}{(s+n)^2 - (p+r)^2} + \frac{n-s}{(n-s)^2 - (p+r)^2} + \frac{s+n}{(s+n)^2 - (p-r)^2} + \frac{n-s}{(n-s)^2 - (p-r)^2} \right)$$

for $p + r + s + n = $ odd, and zero otherwise.

Substituting for R_n and numerically inverting the system of Equation (B.4) leads to the integration weights. Finally, the approximate value of the integrals is calculated from Equation (B.1). The accuracy

of the integration algorithm is demonstrated by considering the infinite integral $I = \int_0^\infty dx\, x e^{-x^2} J_0^2(x)$, with the exact solution of $I = e^{-1/2} I_0(1/2)/2 = 0.3225176352245750$, in which I_0 is the modified Bessel function of the second kind. Its numerical evaluation, with $N = 100$ and $M_i = 8$, with $i = 1, 2, 3$, for $a = 0$ and $b = 10$, and letting $f(x) = 1$, $\chi_1(x) = x e^{-x^2}$ and $\chi_2(x) = \chi_3(x) = J_0(x)$, leads to a value of 0.3225176352245752.

Appendix C

The numerical scheme used to solve a hypersingular integral equation requires an additional constraint equation to achieve a unique solution. However, the nature of the problem does not provide any constraint conditions, as opposed to formulations of the Cauchy type. Furthermore, Equation (23) has a unique solution without any additional constraint equation. Thus, a constraint equation is introduced by multiplying Equation (23), with $r^2(1 - x^2)^{3/2}$, and integrating over x as

$$
\frac{2}{\pi a} \int_{-1}^{1} dt\, g(t) \int_{-1}^{1} dx\, \frac{r^2(1-x^2)^{3/2}}{(t-x)^2} + \frac{1}{2\pi} \int_{-1}^{1} dt\, g(t) \int_{-1}^{1} dx\, \frac{r(1-x^2)^{3/2}}{t-x}
$$
$$
+ \frac{a}{16\pi} \int_{-1}^{1} dt\, g(t) \int_{-1}^{1} dx\, \ln|t-x|(1-x^2)^{3/2} - \frac{a}{8\pi} \int_{-1}^{1} dt\, f^*(t) \int_{-1}^{1} dx\, \ln|t-x|(1-x^2)^{3/2}
$$
$$
+ \int_{-1}^{1} dt\, g(t) \int_{-1}^{1} dx\, M_1(x,t) r^2(1-x^2)^{3/2} + \int_{-1}^{1} dt\, g^*(t) \int_{-1}^{1} dx\, M_2(x,t) r^2(1-x^2)^{3/2}
$$
$$
+ i\frac{\gamma}{2} \int_{-1}^{1} dx\, g(x) r(1-x^2)^{3/2} - i\frac{\gamma}{2} \int_{-1}^{1} dx\, g^*(x) r(1-x^2)^{3/2}
$$
$$
+ i\frac{2\gamma}{a} \int_{-1}^{1} dx\, \frac{dg(x)}{dx} r^2(1-x^2)^{3/2} = \int_{-1}^{1} dx\, \frac{p(r)+iq(r)}{\gamma_{11}} r^2(1-x^2)^{3/2}. \quad \text{(C.1)}
$$

This equation can be further simplified by using the results for the definite integrals of Hadamard and Cauchy types given by Kaya [1984], and the definite integrals of logarithmic type as

$$
\int_{-1}^{1} dt\, \frac{t^n \sqrt{1-t^2}}{(t-x)^2} = \sum_{k=1}^{n+1} k b_k x^{k-1}, \qquad \int_{-1}^{1} dt\, \frac{t^n \sqrt{1-t^2}}{t-x} = \sum_{k=0}^{n+1} b_k x^k,
$$
$$
\frac{1}{\pi} \int_{-1}^{1} dt\, \sqrt{1-t^2}\, \ln|t-x| = \frac{x^2}{2} - \frac{1}{4}(1 + 2\ln 2),
$$
$$
\frac{1}{\pi} \int_{-1}^{1} dt\, t^2 \sqrt{1-t^2}\, \ln|t-x| = \frac{x^4}{4} - \frac{x^2}{4} + \frac{1}{32}(1 - 4\ln 2),
$$

where

$$
b_k = \frac{\sqrt{\pi}}{2} \frac{\Gamma((n-k)/2)}{\Gamma((n-k+3)/2)}
$$

for $n - k =$ odd, and zero otherwise. Finally, this equation can be put into the concise form

$$\int_{-1}^{1} dt\, K_{1c}(t)g(t) + K_{2c}(t)g^{*}(t) = \tilde{g},$$

$$K_{1c}(t) = \frac{a}{512}\left(-3(83 + \ln 16) - 1728t - 552t^2 + 2176t^3 + 1400t^4\right)$$

$$+ i\frac{3}{4}a\gamma\,(1+t)\left(-1 + 2t + 3t^2\right)\sqrt{1-t^2} + \int_{-1}^{1} dx\, M_1(x, t)r^2\left(1-x^2\right)^{3/2}, \quad \text{(C.2)}$$

$$K_{2c}(t) = \frac{a}{256}\left(3(3 + \log 16) + 8t^2(-3 + t^2)\right) - i\frac{a\gamma}{4}(1+t)(1-t^2)^{3/2} + \int_{-1}^{1} dx\, M_2(x, t)r^2(1-x^2)^{3/2},$$

$$\tilde{g} = \int_{-1}^{1} dx\, \frac{p(r) + iq(r)}{\gamma_{11}} r^2(1-x^2)^{3/2}.$$

Note that the multiplying factor, $r^2(1 - x^2)^{3/2}$ is used because it permits simplification of Equation (C.1) by using known definite integrals, which leads to the accurate evaluation of constraint equation. Integration by parts is used to remove the derivative of the unknown function. Integrals appearing in Equation (C.2) can be evaluated accurately using Chebyshev polynomials of second kind [Abramowitz and Stegun 1964].

References

[Abramowitz and Stegun 1964] M. Abramowitz and I. A. Stegun, *Handbook of mathematical functions with formulas, graphs, and mathematical tables*, vol. 55, National Bureau of Standards Applied Mathematics Series, U.S. Government Printing Office, Washington, DC, 1964. MR 29 #4914 Zbl 0171.38503

[Balkan 1995] H. Balkan, *Thin layer with circular debonding over a substrate under either axisymmetric compression or thermal loading*, Ph.D. thesis, University of Arizona, Tucson, AZ, 1995.

[Chan et al. 2003] Y.-S. Chan, A. C. Fannjiang, and G. H. Paulino, "Integral equations with hypersingular kernels: theory and applications to fracture mechanics", *Int. J. Eng. Sci.* **41**:7 (2003), 683–720. MR 2004a:45004

[Erdogan 1965] F. Erdogan, "Stress distribution in bonded dissimilar materials containing circular or ring-shaped cavities", *J. Appl. Mech. (ASME)* **87** (1965), 829–836.

[Erdogan 1969] F. Erdogan, "Approximate solutions of systems of singular integral equations", *SIAM J. Appl. Math.* **17**:6 (1969), 1041–1059. MR 41 #5909 Zbl 0187.12404

[Erdogan 1978] F. Erdogan, "Mixed boundary value problems in mechanics", pp. 1–86 in *Mechanics today*, vol. 4, edited by S. Nemat-Nasser, Pergamon, New York, 1978.

[Erdogan 1997] F. Erdogan, "Fracture mechanics of interfaces", pp. 3–36 in *Proceedings of the First International Conference on Damage and Failure of Interfaces* (Vienna), edited by H.-P. Rossmanith, A. A. Balkema, Rotterdam, 1997.

[Erdogan and Gupta 1971a] F. Erdogan and G. D. Gupta, "Layered composites with an interface flaw", *Int. J. Solids Struct.* **7**:8 (1971), 1089–1107.

[Erdogan and Gupta 1971b] F. Erdogan and G. D. Gupta, "The stress analysis of multi-layered composites with a flaw", *Int. J. Solids Struct.* **7**:1 (1971), 39–61.

[Farris and Keer 1985] T. N. Farris and L. M. Keer, "Williams' blister test analyzed as an interface crack problem", *Int. J. Fract.* **27**:2 (1985), 91–103.

[Goldstein and Vainshelbaum 1976] R. W. Goldstein and V. M. Vainshelbaum, "Axisymmetric problem of a crack at the interface of layers in a multi-layered medium", *Int. J. Eng. Sci.* **14**:4 (1976), 335–352.

[Harding and Sneddon 1945] J. W. Harding and I. N. Sneddon, "The elastic stress produced by the indentation of the plane surface of a semi-infinite elastic body by a rigid punch", *Proc. Camb. Philos. Soc.* **41** (1945), 16–26. MR 6,251e Zbl 0060.42001

[Ioakimidis 1988a] N. I. Ioakimidis, "The hypersingular integrodifferential equation of a straight crack along the interface of two bonded isotropic elastic half-planes", *Int. J. Fract.* **38**:4 (1988), R75–R79.

[Ioakimidis 1988b] N. I. Ioakimidis, "Mangler-type principal value integrals in hypersingular integral equations for crack problems in plane elasticity", *Eng. Fract. Mech.* **31**:5 (1988), 895–898.

[Ioakimidis 1990] N. I. Ioakimidis, "Generalized Mangler-type principal value integrals with an application to fracture mechanics", *J. Comput. Appl. Math.* **30**:2 (1990), 227–234. MR 91d:26003 Zbl 0698.73074

[Jensen 1998] H. M. Jensen, "Analysis of mode mixity in blister tests", *Int. J. Fract.* **94**:1 (1998), 79–88.

[Kabir et al. 1998] H. Kabir, E. Madenci, and A. Ortega, "Numerical solution of integral equations with logarithmic-, Cauchy- and Hadamard-type singularities", *Int. J. Numer. Methods Eng.* **41**:4 (1998), 617–638. Zbl 0905.65127

[Kassir and Bregman 1972] M. K. Kassir and A. M. Bregman, "The stress-intensity factor for a penny-shaped crack between two dissimilar materials", *J. Appl. Mech.* (*ASME*) **39** (1972), 308–310. Trans. ASME 94, Series E.

[Kaya 1984] A. C. Kaya, *Application of integral equations with strong singularities in fracture mechanics*, Ph.D. thesis, Lehigh University, Bethlehem, PA, 1984.

[Kaya and Erdogan 1987] A. C. Kaya and F. Erdogan, "On the solution of integral equations with strongly singular kernels", *Quart. Appl. Math.* **45**:1 (1987), 105–122. MR 88e:45012 Zbl 0631.65139

[Keer et al. 1978] L. K. Keer, S. H. Chen, and M. Comninou, "The interface penny-shaped crack reconsidered", *Int. J. Eng. Sci.* **16**:10 (1978), 765–772. MR 80d:73111 Zbl 0381.73087

[Kilic et al. 2006] B. Kilic, E. Madenci, and R. Mahajan, "Energy release rate and crack surface contact zone by hypersingular integral equations", *Int. J. Solids Struct.* **43**:5 (2006), 1159–1188.

[Lowengrub and Sneddon 1974] M. Lowengrub and I. N. Sneddon, "The effect of internal pressure on a penny-shaped crack at the interface of two bonded dissimilar elastic half-spaces", *Int. J. Eng. Sci.* **12**:5 (1974), 387–396.

[Malyshev and Salganik 1965] B. M. Malyshev and R. L. Salganik, "The strength of adhesive joints using the theory of cracks", *Int. J. Fract. Mech.* **1**:2 (1965), 114–128.

[Miller and Keer 1985] G. R. Miller and L. M. Keer, "A numerical technique for the solution of singular integral equations of the second kind", *Quart. Appl. Math.* **42**:4 (1985), 455–465. MR 87c:65165a Zbl 0593.65094

[Mossakovski and Rybka 1964] V. I. Mossakovski and M. T. Rybka, "Obobshohenie kriteriia Griffitsa–Sneddona na sluchai neodnorodnogo telas", *Prikl. Mat. Mekh.* **28** (1964), 1061–1069. In Russian; translation in *J. Appl. Math. Mech.* **28**:6 (1964), 1277–1286. Zbl 0141.42504

[Muskhelishvili 1992] N. I. Muskhelishvili, *Singular integral equations*, 2nd ed., Dover, New York, 1992. MR 94a:45001 Zbl 0174.16201

[Ozturk and Erdogan 1996] M. Ozturk and F. Erdogan, "Axisymmetric crack problem in bonded materials with a graded interfacial region", *Int. J. Solids Struct.* **33**:2 (1996), 193–219.

[Quan 1991] M. A. Quan, *Analysis of a finite interface crack emitting from the junction of three sectors*, Ph.D. thesis, University of California, Los Angeles, 1991.

[Wan et al. 2003] K.-T. Wan, S. Guo, and D. A. Dillard, "A theoretical and numerical study of a thin clamped circular film under an external load in the presence of a tensile residual stress", *Thin Solid Films* **425**:1 (2003), 150–162.

[Willis 1972] J. R. Willis, "The penny-shaped crack on an interface", *Q. J. Mech. Appl. Math.* **25**:3 (1972), 367–385.

BAHATTIN KILIC: bkilic@email.arizona.edu
Department of Aerospace and Mechanical Engineering, The University of Arizona, Tucson, AZ 85721, United States

ERDOGAN MADENCI: madenci@email.arizona.edu
Department of Aerospace and Mechanical Engineering, The University of Arizona, Tucson, AZ 85721, United States